Nuclear Instruments and Methods in Physics Research A 334 (1993) 328–338
North-Holland

NUCLEAR
INSTRUMENTS
& METHODS
IN PHYSICS
RESEARCH
Section A

Helium gas mixtures for ring imaging Cherenkov detectors with CsI photocathodes

C. Lu, K.T. McDonald and Y. Zhu
Joseph Henry Laboratories, Princeton University, Princeton, NJ 08544, USA

Received 26 January 1993

Use of He gas mixtures at atmospheric pressure (instead of low-pressure hydrocarbon gases) will ease the construction and operation of large-scale parallel-plate RICH detectors with CsI photocathodes. Due to the low density of He gas the number of primary electrons created by minimum-ionizing particles is very small even at atmospheric pressure. Therefore the Cherenkov detector will be nearly blind to ionizing tracks. However, He alone is not a good counting gas; a suitable quenching component must be added for stable operation of the chamber at high gas gain. Five different quenching gases, CH_4, C_2H_6, isobutane, CF_4 and CO_2 have been tested at a mixing ratio of 5%. The first three gas mixtures show very promising performance. The parallel-plate avalanche chamber (PPAC) can be operated up to gains $\approx 5\times10^5$ without secondary avalanches. When the He gas mixture includes 5% of the quenching gas (38 Torr) the efficiency for minimum-ionizing particles is calculated to be $< 20\%$ using a Monte Carlo simulation based on measured gas-gain spectra. Experimental investigation shows that the ratio of the quantum efficiency of a CsI photocathode in an atmospheric-pressure He/i-C_4H_{10} (95/5) gas mixture to that in low-pressure i-C_4H_{10} gas is $\approx 75\%$ for PPAC operation. The effect of mechanical tolerance on uniformity of gas gain at various pressures is also discussed in detail, and He/i-C_4H_{10} (95/5) has the least variation of gain with gap thickness of the mixtures tested.

1. Introduction

In the past few years a readout for Ring-Imaging Cherenkov (RICH) detectors [1] based on CsI photocathodes has been under intensive development [2–15]. The detector is a parallel-plate avalanche chamber (PPAC) with a UV-sensitive solid-CsI photocathode separated by a narrow gap (1–2 mm) from a wire-mesh anode plane (or wire anode plane as in ref. [4]). The Cherenkov light generated in a radiator enters this PPAC through a UV window, passes through the anode mesh, and is detected by the CsI photocathode.

It has been demonstrated that under low pressure (20 Torr of methane, ethane or isobutane) this kind of PPAC can be operated free of photon-feedback breakdown up to very high gas gain [16]. Its simple mechanical structure and easy-to-prepare solid photocathode (CsI does not oxidize [17]) would be very attractive for the high-energy-physics community. A bonus is that the PPAC itself is nearly blind to minimum-ionizing particles because of the low density of the gas [23]. However, it is not easy to construct a practical large-scale PPAC that has low mass, is leak tight and is rigid enough to maintain good gap uniformity. If the PPAC can be operated at atmospheric pressure with stable, high gas gain while remaining blind to minimum-ionizing particles, a workable device should be obtained.

According to this guideline helium is the most promising candidate for the primary chamber gas. First, helium has very low primary ionization, 4.2 primary electrons per cm at 1 atm, in comparison with 25, 41, 84 and 51 for CH_4, C_2H_6, i-C_4H_{10} and CF_4, respectively [18]. Note, however, that a few parts in 10^4 of a molecular gas in in He will increase the ionization by about 40% due to energy transfer from excited states of the He (Penning effect [19]). Even then, the primary ionization remains much lower than in other gases. Second, He is UV transparent, which is essential for a RICH detector. However, this transparency makes He a poor quencher, and hence pure He is unsuitable as a counting gas. Therefore one must search for the best additive for He gas mixtures. Third, in He gas the gas avalanche can start at very low reduced electric field E/P, which means that even at atmospheric pressure the operating voltage of a PPAC is still quite low.

For RICH applications an important issue is the quantum efficiency of the CsI photocathode in a gas-filled chamber. A low-pressure chamber has the advantage that scattering of photoelectrons by the chamber gas back onto the photocathode is minimized [23]. Another subtle issue is the dependence on gas pressure of gas-gain variations due to mechanical variations in the chamber gap.

In this report we summarize experimental and Monte Carlo investigations for five atmospheric-pressure He gas mixtures for possible use in RICH detectors. Detailed comparisons to pure, low-pressure hydrocarbon gases are also presented.

2. Effective ionization coefficient $\bar{\alpha}$ of He gas mixtures

2.1. Experimental setup

When an electron drifts in a gas with a gain coefficient α (= first Townsend coefficient = probability of creating an additional ion pair per unit length) and an attachment coefficient η (= probability of attachment per unit length), then the growth of the avalanche can be described by an effective ionization coefficient $\bar{\alpha} = \alpha - \eta$.

We have measured $\bar{\alpha}$ in five different He gas mixtures with a two-stage parallel-plate avalanche chamber, as shown in fig. 1. The aluminum cathode plate, five field-shaping rings and the stainless-steel ground mesh were connected to a voltage divider to form a uniform-electric-field region 3 cm in length. The open area of these electrodes was 5×5 cm^2.

The second section of the chamber is the 3-mm-long gap surrounded by the ground mesh and the stainless-steel anode mesh (at positive high voltage). The fields in the first section were always much smaller than those in the second section, so the latter was called the "avalanche region", although small avalanches could occur in the first "drift" region as well. The meshes were approximately 80% transparent. Photoelectrons were ejected by UV photons both from the aluminum cathode plane as well as from the ground mesh (which had a thin layer of aluminum evaporated on its surface to enhance its photosensitivity). Even though the aluminized ground mesh had an area 20% of the cathode plane, its observed effective quantum efficiency was only 2.5% that of the ground plane, as the aluminization was extremely thin.

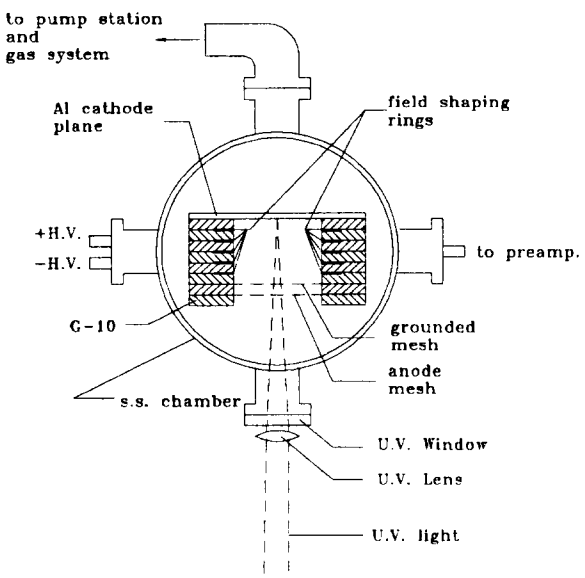

Fig. 1. The two-step parallel-plate avalanche chamber used for measurement of the effective ionization coefficient $\bar{\alpha}$.

The drift chamber was enclosed in a stainless-steel vacuum chamber, which could be pumped down to 10^{-6} Torr. The chamber was illuminated with UV photons through a quartz window. The signal was analyzed by a EG&G ORTEC multichannel analyzer system, which included a model 142PC charge-sensitive preamplifier, a model 570 spectroscopy amplifier, and a model 916 multichannel analyzer. The signal for the preamplifier was taken from the anode wire mesh through a 2000-pF blocking capacitor.

A bench-top gas system was built to mix different gas mixtures. This consisted of an MKS model 147 flow/pressure controller, model 1359 mass-flow controllers, and model 250 valve. The mixed gas went through a Nanochem model L-60 gas filter (designed to remove oxygen, water vapor, and other impurities from methane, ethane, butane, and carbon tetrafluoride) before finally reaching the test chamber. According to the manufacturer, the gas filter is able to eliminate impurities to the few parts per billion range. Because the Nanochem gas filter removes CO_2 as an impurity, the CO_2 gas mixture was directly fed into our chamber without going through the filter.

The pressure in the chamber was monitored with an Edwards model 600A pressure transducer with a quoted resolution of 1 part in 10^4. The water-vapor level in the chamber was monitored with a Kahn Cermet moisture meter. The meter read water-vapor levels in parts per million to a quoted accuracy of approximately ± 4 ppm. The component gases in this study had purity CH_4 99.97%, C_2H_6 99.0%, isobutane 99.5%, CF_4 99.99%, CO_2 99.99% and He 99.997%, according to the vendor. The purity of the gas mixtures as supplied to the chamber was, however, not ascertained, other than the water-vapor content.

2.2. Experimental method and results

In the first part of the study we used a low-intensity deuterium lamp so that we observed only single-electron avalanches. For this the intensity was reduced until the signal rate from the chamber was only 10–1000 Hz. The aluminum cathode was set at ground potential, so there was no electric field between cathode and the ground mesh. Therefore the photoelectrons generated at the cathode were not able to reach the avalanche region (as verified by observing no change in signal when a small positive voltage was applied to the cathode plane). All of the measured events were initiated by the photoelectrons released from the aluminized ground mesh. The spectra were then fitted with the Polya distribution [20],

$$P(g) \propto (fg/G)^{f-1}\, e^{-fg/G},$$

where g is the amplitude (gain) of an avalanche, G is the mean gas gain, and f is a measure of the fluctuation of gas gain: $(\sigma_g/G)^2 = 1/f$. The density-normalized effective ionization coefficient $\bar{\alpha}$ was calculated as $\ln G/ND$, where N is the gas density, and D is the gap length. Typical experimental distributions with their Polya fitting curves for five gas mixtures at 760 Torr pressure are shown in fig. 2.

For values of the effective ionization coefficient $\bar{\alpha}$ near zero (or for some gas mixtures even negative due to electron attachment), it was not possible to use the single-photoelectron method because the signals were too small to be detected and also because the method is blind to primary electrons that become attached. Instead, a second method utilizing both regions of the drift chamber was adopted. The gas pressure of the chamber was set at 20 Torr to make it easier to cover a large range of E/P. The positive high voltage in the avalanche region was fixed for each of the gas mixtures. The electric field in the drift region was then

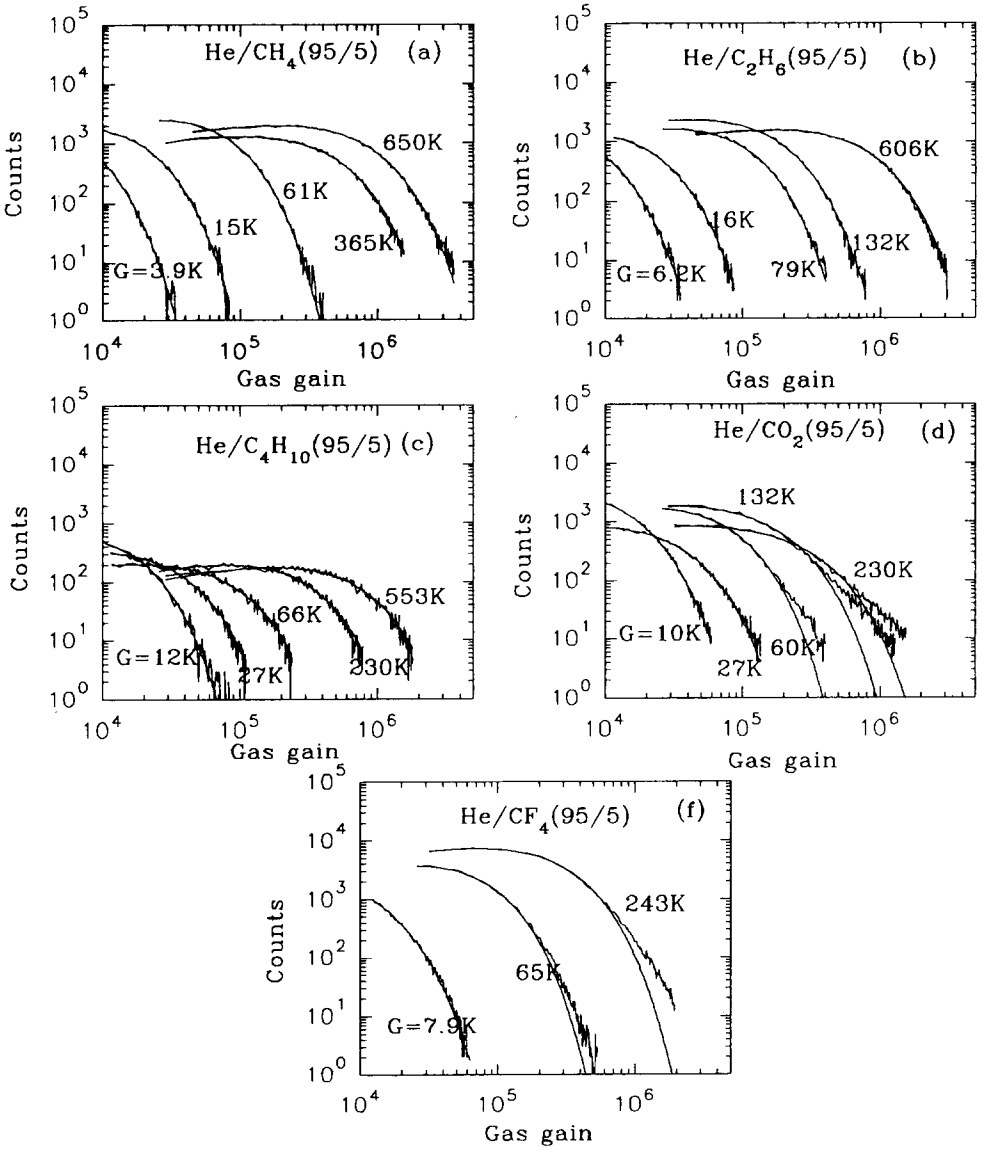

Fig. 2. Single-electron-avalanche distributions with their Polya fittings for He gas mixtures: (a) He/CH_4 (95/5), (b) He/C_2H_6 (95/5), (c) $He/i\text{-}C_4H_{10}$ (95/5), (d) He/CO_2 (95/5), (e) He/CF_4 (95/5). The average gas gains G deduced from the Polya fits are indicated.

varied by adjusting the cathode potential. This ranged from 50 V to the upper limit at which breakdown took place.

For the second measurement the deuterium lamp was replaced by a pulsed N_2 laser, so that a large number of primary electrons were photoemitted during a 1 ns interval. These photoelectrons drifted across the first gap of the chamber and, according to the value of E/P, different numbers fell victim to the attachment process before entering the second gap. The size of the avalanche produced in the second gap varied linearly with the number of entering electrons, since the gain in this region was held constant.

Some primary electrons were ejected from the aluminized ground mesh, and were not subject to the possible attachment in the first gap that we wish to study. The resulting small ($\approx 2.5\%$), constant signal was subtracted from the total, which could then be interpreted in terms of $\bar{\alpha}$ for the first gap.

The region of E/P studied in the second method

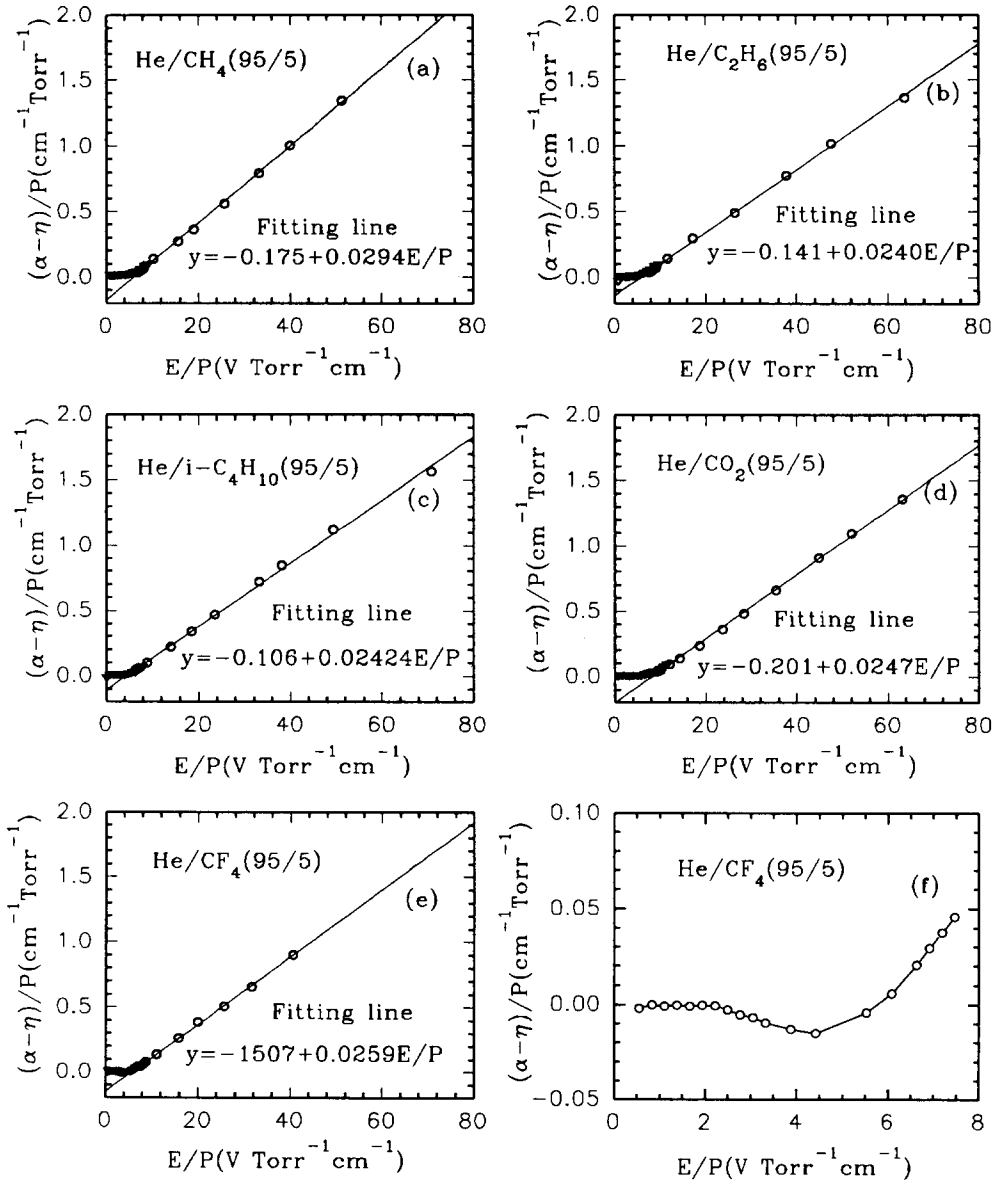

Fig. 3. Effective ionization coefficient $\bar{\alpha}$ for He gas mixtures: (a) He/CH_4 (95/5), (b) He/C_2H_6 (95/5), (c) $He/i\text{-}C_4H_{10}$ (95/5), (d) He/CO_2 (95/5), (e, f) He/CF_4 (95/5).

was partially overlapped by data points measured with the single-photoelectron method. This overlap region served as the normalization for the second method.

The measured effective ionization coefficients $\bar{\alpha}$ for the five gas mixtures are shown in fig. 3. Except for the CF_4 gas mixture, all of the other four mixtures show no electron attachment. Above a certain value of E/P, which depends on the gas mixture, $\bar{\alpha}$ has nearly linear dependence on E/P. The fitting lines are also shown in the figures.

2.3. Discussion

In fig. 2 clear evidence of secondary avalanche dues to UV-photon feedback can be seen for the He/CO_2 and He/CF_4 gas mixtures. When the average gas gain was higher than $\approx 6 \times 10^4$, the measured spectrum deviated from Polya distribution at the high-gain region. We interpret this excess at high gain as due to secondary avalanches that become probable once the initial avalanche is big enough [21]. We calculated the fraction U of the spectrum that exceeded the Polya fit as a measure of the chamber's instability. For He/CO_2 with average gain $\approx 6 \times 10^4$, $U = 2.4\%$, and gain $\approx 2.3 \times 10^5$, $U = 4.9\%$. For He/CF_4 with average gain $\approx 6 \times 10^4$, $U = 1.5\%$, and gain $\approx 2.4 \times 10^5$, $U = 3.3\%$. For the other three gas mixtures there was no indication of the deviation up to average gain $\approx 5 \times 10^5$. Therefore these $He + CH_4$, $+C_2H_6$, and +isobutane are good gas mixtures with regards to stability against photon feedback.

The He/CF_4 gas mixture shows small electron attachment within an E/P range of 2–6 V/(Torr cm), where $\bar{\alpha}$ becomes negative. For a PPAC configuration this is not a problem because we always set E/P at higher values to produce a large signal. For the other four gases there is no electron attachment.

3. Detection efficiency for minimum-ionizing particles of a PPAC with He gas mixtures

A Monte Carlo program has been written to simulate the response of a PPAC filled with He gas mixtures to minimum-ionizing particles.

The number of primary electrons created by a minimum-ionizing particle was taken from ref. [18] for pure He and four other pure gases. The cluster-size distribution was measured by Fischle et al. [22]. From this distribution we can calculate the average number of electrons per cluster. Then knowing the number of primary electrons and average cluster size we infer the average number of primary clusters per unit track length, and hence the mean free path between clusters.

Each of the primary electrons will initiate an avalanche. The average gas gain G for this electron can be calculated according to its position in the PPAC via the effective ionization coefficient $\bar{\alpha}$ measured above. The fluctuations about the average gain are described by a Polya distribution with measured parameter G. The data shown in fig. 2 indicate that at 760 Torr the other Polya-fit parameter f was around 1.5 for all of the gas mixtures tested, and this value was used in our Monte Carlo calculation.

A threshold for detection of a minimum-ionizing particle was set in the calculation at a certain percentage of the average gas gain for a 2-mm-gap PPAC. Fig. 4 shows the calculated detection efficiency for 12 threshold settings from 0 to 100% of the average gas gain. In the same figure we also plot the effect of the

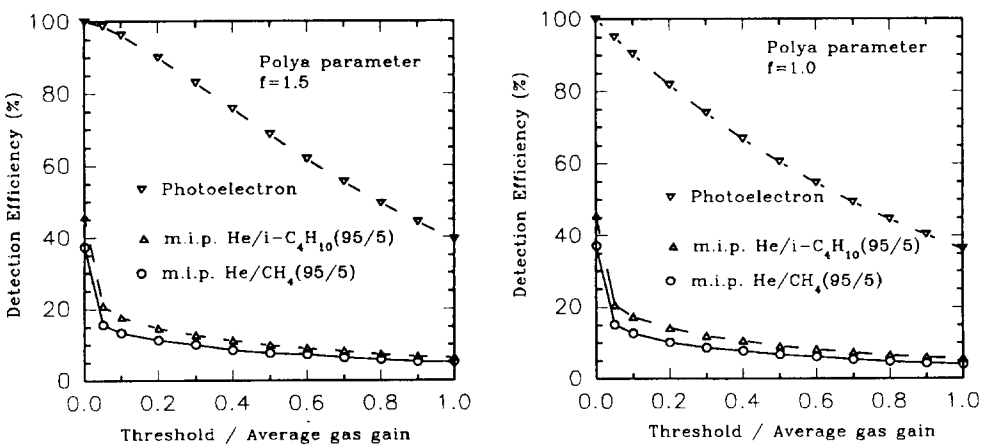

Fig. 4. Calculated detection efficiency of a parallel-plate avalanche chamber for minimum-ionizing particles and single-photoelectrons. The two plots differ only in the value of the Polya-fit parameter f, which is a measure of the fluctuation of the gas gain. The data of fig. 2 are well fit by $f = 1.5$.

threshold cut on single-photoelectron detection efficiency. For this the photoelectron always emerges from the photocathode and crosses the entire gap of the PPAC.

We see from fig. 4 that a threshold set at 5–10% of the average gain for single photoelectrons retains good efficiency for these, while being only about 20% efficient for minimum ionizing particles.

4. Quantum efficiency of CsI photocathodes in atmospheric He gas mixtures and low-pressure hydrocarbon gases

4.1. Measurement of the relative photo electron collection efficiency

One of the advantages of using a low-pressure hydrocarbon gas to detect the photoelectrons from photocathode in a PPAC is its higher photoelectron collection efficiency, according to Anderson et al. [23]. The conclusion was: for efficient collection of photoelectrons, use an organic gas at as low a pressure as possible to minimize the backscattering of photoelectrons onto the cathode. To understand this effect better, we have measured the relative collection efficiency for He/isobutane (95/5) at several gas pressures from 760 down to 100 Torr, with the same setup as in fig. 1.

Single-photoelectron spectra were recorded for several different gas pressures and cathode voltages. The UV light source was a constant-intensity deuterium lamp, attenuated until the counting rate in the detector was less than 1000 Hz. As the gas pressure was varied the positive high voltage on the anode was adjusted to maintain a constant value of the gas gain. Then the event rate in each case should be a direct indication of the photoelectron collection efficiency. The experimental results of event rate vs E/P are summarized in fig. 5 together with fitting curves according to Thomson's theory [24] as discussed below.

4.2. Comparison with a model calculation

According to a modified version of Thomson's theory applicable near a photocathode [25], there are two competing processes that govern the motion of emitted electron. Near the cathode the random electron speed is v_0 corresponding to the initial velocity of electron emission from the electrode, and due to the elastic collisions with the gas molecules the electrons' directions are randomized. Therefore some of the emitted electrons will diffuse back to cathode. The second process is the drift of electrons under the electric field towards to the anode.

The ratio of total current density j received at anode to the vacuum photoelectric current density j_0 at the cathode is deduced to be [24]

$$R = j/j_0 = \frac{4v_{\text{drift}}}{\bar{v}_0 + 4v_{\text{drift}}}.$$

At very low E/P, we can assume that the electron drift velocity is nearly proportional to E/P. Writing $v_{\text{drift}} \approx \kappa E/P$, where κ is the reduced electron mobility in the gas, we have

$$R = j/j_0 = \frac{a(E/P)}{1 + a(E/P)}, \qquad \text{where } a = \frac{4\kappa}{\bar{v}_0}.$$

In the experiments described above the value of the vacuum photoelectric current density is not known, but the data shown in fig. 5 determine that $a \approx 3$ cm Torr/V.

Certainly the qualitative character of the data is well described by the model. That is, backscattering and consequent loss of photoelectrons is prominent unless the electric field on the cathode is larger than a characteristic value, which for a gas of interest, He/isobutane (95/5) proves to be $E/P \gtrsim 1$ V/(cm Torr).

For large E/P the electron drift velocity no longer varies linearly with E/P but typically saturates at

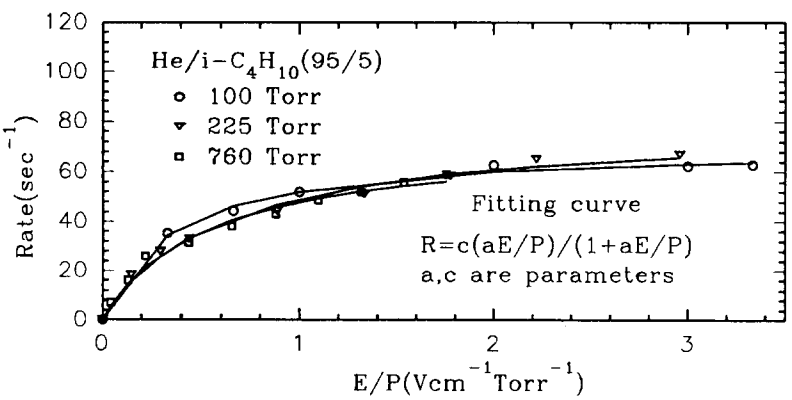

Fig. 5. Relative photoelectron collection efficiency vs E/P for He/isobutane (95/5).

some value v_{sat}. The model then predicts that there will be a maximum photoelectron collection efficiency

$$R_{max} = \frac{4v_{sat}}{\bar{v}_0 + 4v_{sat}}.$$

The value of v_{sat} for He/i-C_4H_{10} (95/5) has not been measured, but the value $v_{sat} = 2$ cm/μs has been reported for the closely related mixture He/i-C_4H_{10}/TMAE ($93/7/5 \times 10^{-4}$) [26]. We estimate $\bar{v}_0$ as that due to the electron's thermal motion, $\bar{v}_0 = \sqrt{kT/m_e} = 6.8$ cm/μs, leading to a collection efficiency $R_{max} \approx 0.5$.

According to this simple picture gas mixtures with a fast drift velocity will have a higher photoelectron collection efficiency. This argument is a good approximation only for those gases that have a widely spaced energy-level structure such as H_2 and He, so that collisions with the drift electrons are likely to be elastic. Organic gases have a more complicated level structure, resulting in inelastic collisions with drift electrons and a correspondingly smaller backscattering cross section. Indeed, as recently reported by Anderson et al. [14], the quantum efficiency of a CsI photocathode in a methane or ethane atmosphere is even higher than in vacuum. This suggests that not only is the backscattering loss low in these gases, but there is a surface effect that enhances the extraction of photoelectrons.

These arguments imply that He gas mixtures may not be optimal for collection of photoelectrons, and so we performed measurements of the quantum efficiency of CsI cathodes at various gas pressures.

4.3. Measurement of the pressure dependence of quantum efficiency

The quantum efficiency of CsI cathodes can be measured by comparison to that of TMAE gas, which has a similar dependence of quantum efficiency on wavelength and whose absolute quantum efficiency has been determined by Holroyd et al. [27]. The apparatus used in our measurement is shown in fig. 6, and is based on a design of Hoeneisen et al. [5] of a double-gap chamber that can be used with either a CsI photocathode or TMAE photosensitive gas.

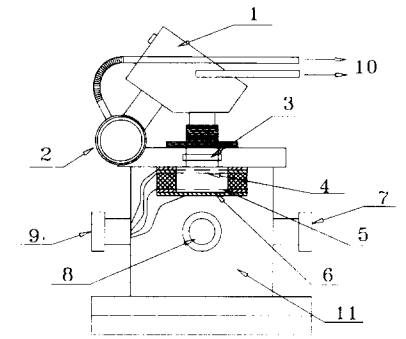

1. Monochromator;
2. Hydrogen lamp;
3. UV window;
4. Mesh;
5. Anode mesh;
6. Photocathode;
7. Vacuum port;
8. Gas port;
9. Signal & H.V. port;
10. To nitrogen gas bottle;
11. S.S. vacuum chamber.

Fig. 6. The test chamber for measurement of the quantum efficiency of CsI photocathodes in a parallel-plate avalanche chamber operated with various gases.

UV light is derived from a pulsed (≈ 400 Hz) hydrogen lamp (Hamamatsu) and the desired wavelength selected with a monochromator (Instruments SA model H1060). For studies near 170-nm wavelength, the cut-off of UV-grade quartz, all light paths must be in nitrogen. The chamber was pumped down with a Balzers TSH180 oil-free molecular-drag/diaphragm pump system to 5×10^{-6} Torr using a LN_2 cold trap. The chamber was baked at 60°C every night between data

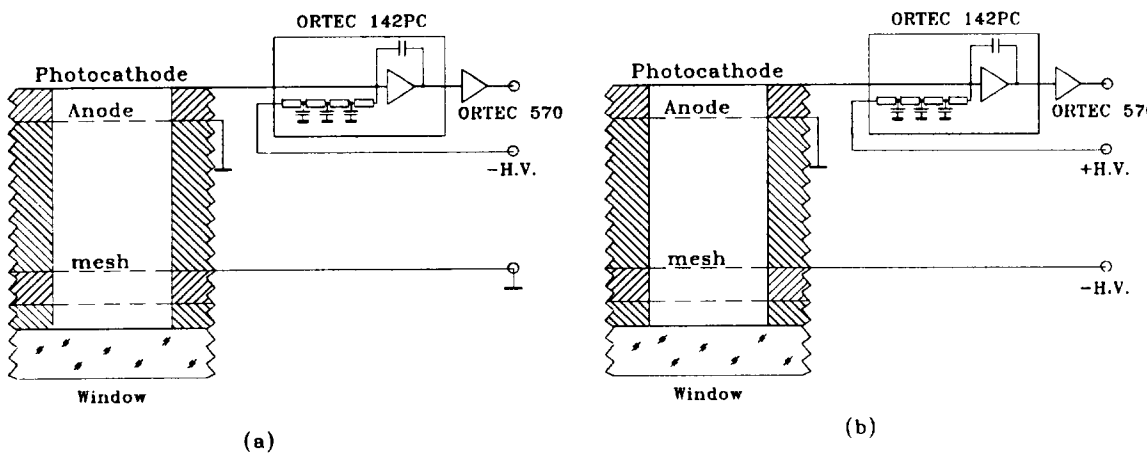

Fig. 7. The high voltage arrangement for quantum-efficiency measurement: (a) CsI photocathode mode; (b) TMAE mode.

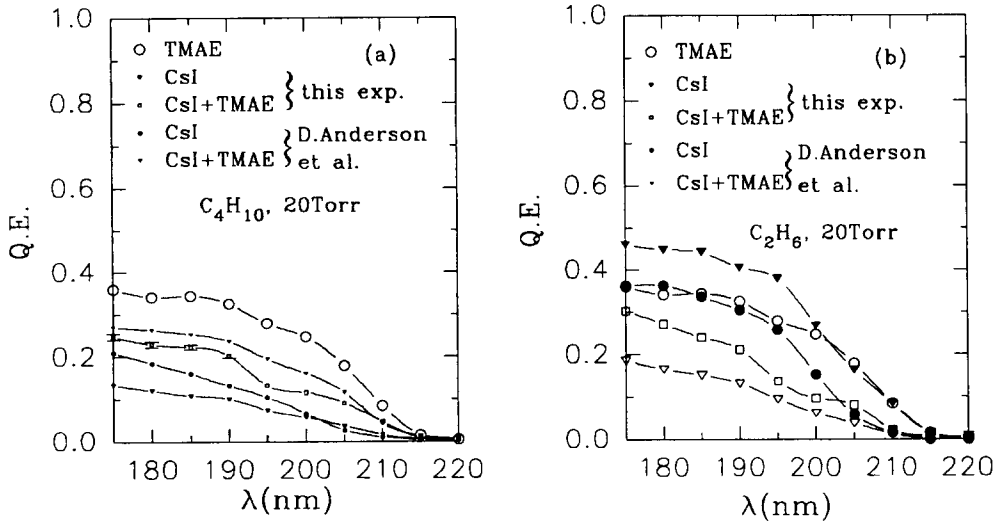

Fig. 8. The quantum efficiency of CsI (a) in C_2H_6, and (b) in i-C_4H_{10}. Also shown are data points from Anderson et al. [14].

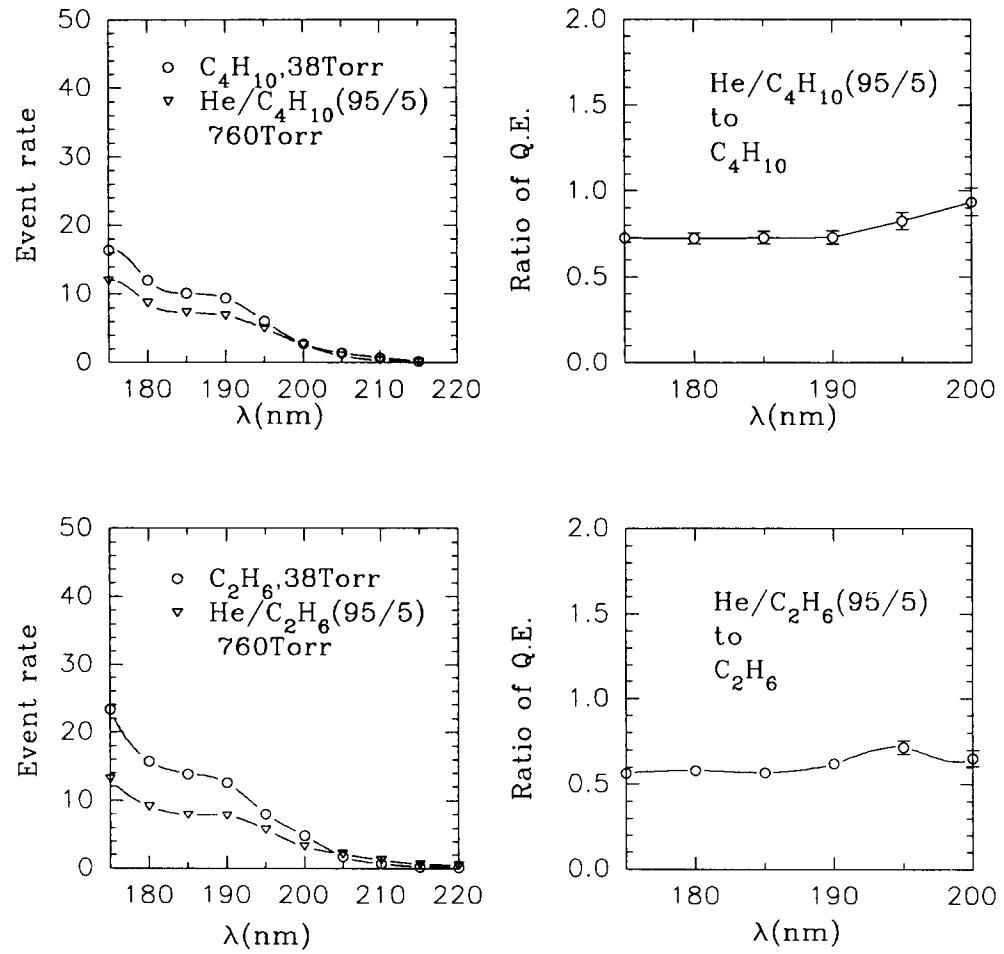

Fig. 9. Comparison of the quantum efficiency CsI photocathodes for He gas mixtures at atmospheric pressure and pure hydrocarbon gases at low pressure.

runs, and the photocathode could also be heated to 60°C by a flexible Kapton heating pad (Omegalux KHLV101-10) attached to the back side of the photocathode. Data were taken only after a few days of baking at which time the moisture level inside the chamber was less than 1 ppm, the lower limit of sensitivity of our Kahn Cermet hygrometer. All of the hydrocarbon gases used in this study were scientific grade (MG Industries) with minimum purity: methane 99.9995%, ethane 99.95%, isobutane 99.96% and helium 99.999%. The hydrocarbon gas was admitted to the chamber through Oxisorb (MG Industries); according to manufacturer's specification the discharge gas purity should be < 0.1 ppm O_2 and < 0.5 ppm H_2O when used with scientific-grade gases.

For measurement of the relative quantum efficiency of the CsI photocathode, it was held at negative high voltage and the anode mesh was grounded as shown in fig. 7a. The chamber was filled with a gas mixture and the event rate recorded when varying the wavelength of the monochromator from 170 to 220 nm. The trigger rate of the hydrogen lamp was also recorded. The output of the hydrogen lamp was attenuated by an iris until the event rate was less than one out of 10 triggers. Thus we studied the effect of single photons in over 90% of the events.

We next measured the relative quantum efficiency of TMAE gas. For this the CsI-coated electrode was used as an anode and was set at positive high voltage as shown in fig. 7b. The wire mesh that previously served as the anode remained grounded, but now functioned as a grid. The other wire mesh, which previously played no role, was now set at -250 V. The 2.03-cm-thick region between this mesh and the grounded mesh served as the photodetection and transfer area. TMAE vapor was admitted into the evacuated chamber until the vapor pressure reached ≈ 400 mTorr. Then the chamber was filled with hydrocarbon gas to the desired pressure. UV photons were absorbed by TMAE vapor, converted to photoelectrons, and drifted towards the grounded mesh without significant multiplication in the weak electric field. After passing through the grounded mesh they entered the avalanche region and were subsequently detected at the anode.

The photon absorption spectrum of TMAE is rather flat from 170 to 220 nm [27], and we took the average value of the absorption coefficient μ to be 0.488/cm for 400 mTorr TMAE. From the geometry of our test chamber and transparency of the meshes we calculated the portion of UV light absorbed by the TMAE vapor in the transfer region. Using the known quantum efficiency of TMAE [27] and the ratio of the event rates of CsI mode and TMAE mode in the test chamber, the quantum efficiency of CsI photocathode was derived. The results are summarized in fig. 8.

In a third set of measurements the quantum efficiency of CsI photocathodes with an adsorbed layer of TMAE was determined. For this we started with the TMAE-mode measurements, and then restored the electrodes to the CsI-mode configuration without changing the chamber gas. Photoelectrons produced in the transfer region did not produce avalanches in this configuration. A correction was made for the substantial attenuation of the UV light in the transfer region, thereby deriving the quantum efficiency for CsI + TMAE cathodes also reported in fig. 8.

Fig. 9 presents comparisons of the quantum efficiency of CsI photocathodes in low-pressure hydrocarbon gas and atmospheric-pressure mixtures of helium and hydrocarbon gas of the same partial pressure. The average ratio of quantum efficiency for He/C_2H_6 (95/5) to C_2H_6 is about 0.55, and for $He/i\text{-}C_4H_{10}$ to $i\text{-}C_4H_{10}$ is about 0.75. Thus the He/isobutane mixture causes relatively small loss of photoelectrons and remains a good candidate for atmospheric-pressure operation.

5. The relation of mechanical tolerance to gas gain

Variation of gas gain in a large-area, narrow-gap parallel-plate avalanche chamber due to variation in the chamber gap could be a serious drawback. In a PPAC the Townsend coefficient a is constant through-

Table 1
Effect of a change in gap thickness of $\delta D = 100$ μm on the gas gain for different gases and pressures. Parameter a is from fits to the data of figs. 3 and 10 of the form $\alpha/P = a + bE/P$

Gas	a	b	$(E/P)_{min}$ [V/cm Torr]	P [Torr]	G_2/G_1
He/CH_4 (95/5)	−0.175	0.0294	5.95	760	0.26
He/C_2H_6 (95/5)	−0.141	0.0240	5.87	760	0.34
$He/i\text{-}C_4H_{10}$ (95/5)	−0.106	0.0242	4.37	760	0.45
He/CO_2 (95/5)	−0.201	0.0247	8.14	760	0.22
He/CF_4 (95/5)	−0.151	0.0259	5.82	760	0.32
C_2H_6	−1.532	0.0273	56.1	20	0.74
$i\text{-}C_4H_{10}$	−2.580	0.0287	89.9	20	0.60

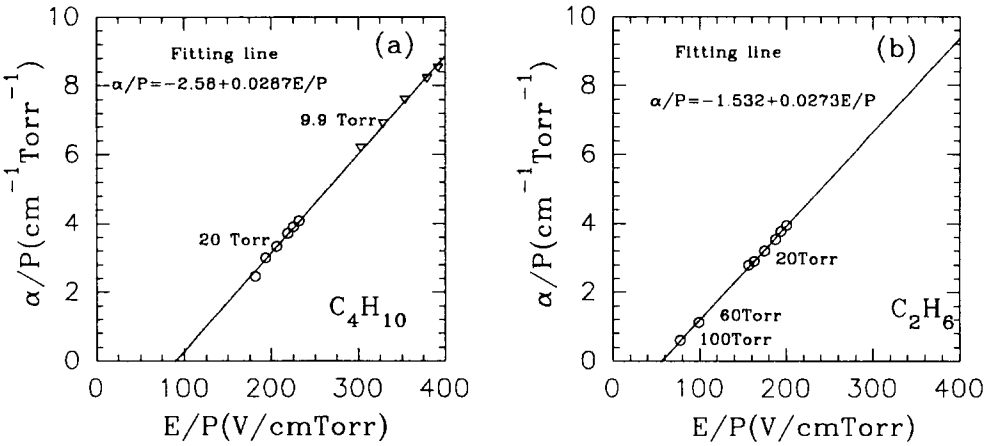

Fig. 10. The reduced Townsend coefficient of C_2H_6 and i-C_4H_{10}.

out the chamber and the gas gain can be written $G = e^{\alpha D}$, where D is the gap thickness. We have seen in fig. 3 that for gases of interest the reduced Townsend coefficient α/P is well described by a linear fit: $\alpha/P = a + bE/P$. In this case the gain becomes

$$G = e^{aPD+bV},$$

where V is the voltage between the anode and cathode. Therefore the ratio of the gas gains in regions of differing gas thickness is

$$G_2/G_1 = e^{aP(D_2-D_1)} = e^{aP\delta D},$$

where G_1 and G_2 are the gas gains for gaps of D_1 and D_2, respectively.

Thus with gases for which the reduced Townsend coefficient behaves as $\alpha/P = a + bE/P$ it is clearly desirable that a be small. Among the five gas mixtures surveyed the best in this respect is He/isobutane (95/5), as summarized in table 1. For example, a 100-μm variation in the chamber gap would lead to a factor of two change in gas gain. Because parameter a is negative in the fits to α/P there is no gas gain until E/P is greater than $-a/b$, which is given as $(E/P)_{min}$ in table 1.

It is interesting to compare atmospheric-pressure gas mixtures to low-pressure gases with regards to their gain sensitivity to gap thickness. For this we made additional measurements for C_2H_6 and isobutane using the method of section 2 above. Results are shown in fig. 10 and also in table 1. While the low-pressure gases are superior to atmospheric-pressure mixtures with regard to gain stability against gap variation the advantage over He/isobutane (95/5) is not overwhelming.

6. Conclusions

- A PPAC filled with 760 Torr of He/CH_4, He/C_2H_6, He/i-C_4H_{10} with a 95/5 mixing ratio can reach a gas gain higher than 5×10^5 without instability due to secondary avalanches.
- The detection efficiency for single photoelectrons in such a PPAC will be higher than 95% if the electronics threshold is less than 10% of the average signal.
- For a 2-mm-gap PPAC filled with these He gas mixtures, the detection efficiency for minimum-ionizing particles is below 20% for any electronics threshold greater than 10% of the average single-photoelectron signal.
- The quantum efficiency of CsI photocathode is certainly affected by the gas environment. The quantum efficiency of He/i-C_4H_{10} (95/5) at 760 Torr is about 75% of pure i-C_4H_{10} at low pressure.
- Variation in gas gain due to variation in chamber-gap thickness should not pose a severe difficulty for He gas mixtures at atmosphere pressure or pure hydrocarbon gases at low pressure.

Acknowledgements

We would like to thank David Anderson, Nigel Lockyer, Jorge Millan, Vladimir Peskov and Tom Ypsilantis for stimulating conversations. This work was supported in part by the U.S. Department of Energy grant DE-FG02-91ER40671 and by the Texas National Research Laboratory Commission grant RGFY9235.

References

[1] J. Séguinot and T. Ypsilantis, Nucl. Instr. and Meth. 142 (1977) 377.
[2] V. Peskov et al., Nucl. Instr. and Meth. A269 (1988) 149.
[3] V. Dangendorf et al., Nucl. Instr. and Meth. A289 (1990) 322.
[4] J. Seguinot et al., Nucl. Instr. and Meth. A297 (1990) 133.

[5] B. Hoeneisen, D.F. Anderson and S. Kwan, Nucl. Instr. and Meth. A302 (1991) 447.
[6] G. Charpak et al., Nucl. Instr. and Meth. A307 (1991) 63.
[7] V. Dangendorf et al., Nucl. Instr. and Meth. A308 (1991) 519.
[8] G. Charpak et al., Nucl. Instr. and Meth. A310 (1991) 128.
[9] S. Kwan and D.F. Anderson, Nucl. Instr. and Meth. A309 (1991) 190.
[10] Y. Giomatris et al., Nucl. Instr. and Meth. A323 (1992) 431.
[11] G. Charpak, V. Peskov and F. Sauli, Nucl. Instr. and Meth. A323 (1992) 445.
[12] H. Ehrlichmann, E. Michel and P. Križan, Nucl. Instr. and Meth. A323 (1992) 452.
[13] M. Starič et al., Nucl. Instr. and Meth. A323 (1992) 457.
[14] D.F. Anderson et al., Nucl. Instr. and Meth. A323 (1992) 626.
[15] N.S. Lockyer et al., Nucl. Instr. and Meth. A332 (1993) 142.
[16] A. Breskin, Nucl. Instr. and Meth. 196 (1982) 11.
[17] A.H. Sommer, Photoemissive Materials (Wiley, New York, 1968).
[18] J. Va'vra, Nucl. Instr. and Meth. A323 (1992) 34.
[19] W.P. Jesse and J. Sadauskis, Phys. Rev. 100 (1955) 1755.
[20] J. Byrne, Proc. Roy. Soc. Edin. 66A (1962) 33.
[21] J. Byrne and F. Shaikh, Nucl. Instr. and Meth. 79 (1970) 286.
[22] H. Fischle et al., Nucl. Instr. and Meth. A301 (1991) 202.
[23] D.F. Anderson et al., Nucl. Instr. and Meth. 217 (1983) 217.
[24] L.B. Loeb, Basic Processes of Gaseous Electronics (University of California Press, Berkeley and Los Angeles, 1955) p. 601.
[25] S.C. Brown, Basic Data of Plasma Physics (The Technology Press of M.I.T. and John Wiley and Sons, Inc., New York, 1959) p. 99.
[26] A. Peisert and F. Sauli, CERN 84–08 (13 July, 1984) p. 54.
[27] R.A. Holroyd et al., Nucl. Instr. and Meth. A261 (1987) 440.